



A local meshless method for time fractional nonlinear diffusion wave equation

Alpesh Kumar¹ · Akanksha Bhardwaj¹

Received: 3 October 2018 / Accepted: 12 December 2019 / Published online: 4 January 2020
© Springer Science+Business Media, LLC, part of Springer Nature 2020

Abstract

We present a radial basis function-based local collocation method for solving time fractional nonlinear diffusion wave equation. The main beauty of the local collocation method is that only the nodes located in the subdomain, surrounding the local collocation point, need to be considered when we are calculating the numerical solution at this point. We also prove the unconditional stability and convergence of the proposed scheme. Some numerical experiments are carried out and numerical results are compared with an analytical solution to confirm the efficiency and reliability of the proposed method.

Keywords Radial basis function · Local collocation · Time fractional · Diffusion wave equation

1 Introduction

In the last few decades, there has been growing interest observed in fractional calculus due to its capabilities to model various phenomenon in the fields of applied science, physics, engineering, and finance [1, 3, 5, 6]. The wide applicability of fractional equations attract the researcher to find its reliable and accurate solutions using the suitable technique such as collocation method [33], finite difference method [19, 41, 44], collocation method [2], finite element method [11, 27], spectral method [17], element-free Galerkin (EFG) method [7], and homotopy analysis method [15].

✉ Akanksha Bhardwaj
pmth17001@rgipt.ac.in; bhardwaj.ak11@gmail.com

Alpesh Kumar
alpeshk@rgipt.ac.in; alpeshmath@gmail.com

¹ Department of Basic Sciences and Humanities, Rajiv Gandhi Institute of Petroleum Technology, Amethi 229304, India

In last two decades, special attention has been devoted to solving differential equations by meshfree methods, more precise methods based on radial basis function (RBF). The main feature of the method is they avoid the use of meshes hence known as meshfree and applicable on irregular domain as well. In [30], Mardani et al. developed meshless method for time fractional advection-diffusion equation with variable coefficients, Wen Chen et al. [5] developed Kansa method for time fractional diffusion equations, Yang et al. [43] developed MLS meshless method for time fractional diffusion-wave equation, Dehghan et al. [14] developed element-free Galerkin method for time fractional diffusion wave equation, Dehghan et al. [12] presented collocation method for time fractional nonlinear sine-Gordon and Klein-Gordon equations, Salehi [35] introduced meshless point collocation method for multiterm diffusion wave equation, Tayebi et al. [39] presented meshless methods for solving two-dimensional variable-order time fractional advection-diffusion equation, Hosseini et al. [25] solve fractional telegraph equation by using radial basis functions collocation method, Pinghui, et al. [45] extended meshless MLS method for time-dependent fractional advection-diffusion equations, Liu et al. [29] presented collocation method for time fractal mobile/immobile transport model, and Sun et al. [37] presented an fast Kansa collocation method for spatiotemporal fractional diffusion equation. For more application of meshfree method refer [4, 8, 9, 20, 22–24, 31, 32, 40, 42] and references therein. Generally, the global version of meshfree method suffered the stability issue and in fact there is trade off observation in RBF collocation method. To avoid these issue, several local versions of meshfree methods are proposed. In [28], Kumar et al. presented local collocation method for time fractional diffusion wave equation, Ghehsareh et al. [21] presented local weak form meshless method to simulate a variable order time-fractional mobile-immobile transport model, and Hosseini et al. [26] presented a local radial point interpolation (MLRPI) method for solving time fractional diffusion-wave equation with damping term. The selection of optimal shape parameter is not an easy task, during the implementation of the collocation method, but there are some strategies are available for selecting suitable value of the shape parameter in local RBF base methods, for more details, we refer Sarra [36], Dehghan [10, 13, 16, 18], and reference therein.

In this paper, we consider the following fractional diffusion-wave equation

$$\begin{cases} {}_0^c \mathcal{D}_t^\alpha u(\mathbf{x}, t) = \Delta u(\mathbf{x}, t) - F(u(\mathbf{x}, t)) + f(\mathbf{x}, t), & (\mathbf{x}, t) \in \Omega \times (0, T], \\ u(\mathbf{x}, 0) = \xi(\mathbf{x}), \quad \frac{\partial u(\mathbf{x}, 0)}{\partial t} = \psi(\mathbf{x}), & \mathbf{x} \in \Omega \\ u(\mathbf{x}, t) = 0, & \mathbf{x} \in \partial\Omega, \end{cases} \tag{1}$$

where $T > 0$, $1 < \alpha < 2$, and $f(\mathbf{x}, t)$ is sufficiently smooth function. The function $F(u(\mathbf{x}, t))$ satisfies the Lipschitz condition with respect $u(\mathbf{x}, t)$ with Lipschitz constant L . Furthermore for any positive integer k , the ${}_0^c \mathcal{D}_t^\alpha u(\mathbf{x}, t)$ is Caputo’s differential operator define as

$${}_0^c \mathcal{D}_t^\alpha u(\mathbf{x}, t) = \begin{cases} \frac{1}{\Gamma(k - \alpha)} \int_0^t \frac{\partial^k u(\mathbf{x}, s)}{\partial s^k} \frac{ds}{(t - s)^{\alpha - (k-1)}}, & k - 1 < \alpha < k, \\ \frac{\partial^k u(\mathbf{x}, t)}{\partial t^k}, & \alpha = k. \end{cases} \tag{2}$$

In present work, a meshless radial basis function-based local collocation method for spatial approximation and a finite difference approximation for Caputo’s time derivatives is employed for numerical solution of time fractional nonlinear diffusion wave equation presented.

The rest of this paper is organized as follows: In Section 2, time discretization scheme is presented; furthermore, this section is also devoted to prove the stability and convergence of the numerical scheme in semi-discrete form. Section 3 give us brief discussion of local collocation method and numerical implementation of the proposed method. In Section 4, we did some numerical experiments on test problems and provide computational results to prove the efficiency and accuracy of the proposed method. Finally, Section 5 end with some concluding remark.

2 The time discretization

This section devoted for development and analysis of time semi-discretization of the proposed problem (1).

The Caputo’s fractional derivative ${}^c_0\mathcal{D}_t^\alpha u(\mathbf{x}, t)$ could be rewritten as follows

$${}^c_0\mathcal{D}_t^\alpha u(\mathbf{x}, t) = \begin{cases} \frac{1}{\Gamma(2-\alpha)} \int_0^t \frac{\partial^2 u(\mathbf{x}, s)}{\partial s^2} \frac{ds}{(t-s)^{\alpha-1}}, & 1 < \alpha < 2, \\ \frac{\partial^2 u(\mathbf{x}, t)}{\partial t^2}, & \alpha = 2. \end{cases} \tag{3}$$

For any positive integer N , we let $\delta t = \frac{T}{N}$, be the time step, and $t_n = n\delta t$, $n = 0, 1, \dots, N$ be temporal mesh points.

Let us introduced the notation $u^{n-\frac{1}{2}} = \frac{1}{2}(u^n + u^{n-1})$, and $\delta_t u^{n-\frac{1}{2}} = \frac{1}{\delta t}(u^n - u^{n-1})$, where u^n is the abbreviation of $u(\mathbf{x}, t_n)$.

Lemma 1 Suppose $1 < \alpha < 2$, and $g(t) \in C^2[0, T]$, it holds that

$$\int_0^{t_n} g'(s)(t_n - s)^{1-\alpha} ds = \sum_{k=1}^n \frac{g(t_k) - g(t_{k-1})}{\delta t} \int_{t_{k-1}}^{t_k} (t_n - s)^{1-\alpha} ds + R^n, \quad 1 \leq n \leq N \tag{4}$$

and

$$|R^n| \leq \left(\frac{1}{2(2-\alpha)} + \frac{1}{2} \right) \delta t^{3-\alpha} \max_{0 \leq t \leq t_n} |g''(t)|. \tag{5}$$

Proof See [38]. □

Lemma 2 Let $1 < \alpha < 2$, $a_0 = \frac{1}{\delta t \Gamma(2-\alpha)}$, and $b_k = \frac{\delta t^{2-\alpha}}{(2-\alpha)} [(k+1)^{2-\alpha} - (k)^{2-\alpha}]$, $k = 0, 1, 2, \dots$, then

$$\left| \frac{1}{\Gamma(2-\alpha)} \int_0^{t_n} \frac{g'(s)}{(t_n-s)^{\alpha-1}} ds - a_0 \left[b_0 g(t_n) - \sum_{k=1}^{n-1} (b_{n-k-1} - b_{n-k}) g(t_k) - b_{n-1} g(0) \right] \right| \leq \frac{1}{\Gamma(2-\alpha)} \left(\frac{1}{2(2-\alpha)} + \frac{1}{2} \right) \delta t^{3-\alpha} \max_{0 \leq t \leq t_n} |g''(t)|. \tag{6}$$

Proof See [38]. □

Lemma 3 Let $1 < \alpha < 2$, and $b_k = \frac{\delta t^{2-\alpha}}{(2-\alpha)} [(k+1)^{2-\alpha} - (k)^{2-\alpha}]$, $k = 0, 1, 2, \dots$, then

$$b_0 > b_1 > b_2 > \dots > b_k \rightarrow 0, \text{ as } k \rightarrow \infty.$$

Proof See [38]. □

Now let us define

$$v(\mathbf{x}, t) = \frac{\partial u(\mathbf{x}, t)}{\partial t} \tag{7}$$

$$w(\mathbf{x}, t) = \frac{1}{\Gamma(2-\alpha)} \int_0^t \frac{\partial v(\mathbf{x}, s)}{\partial s} \frac{ds}{(t-s)^{\alpha-1}}. \tag{8}$$

Now application of Taylor expansion and (7) yields

$$v^{n-\frac{1}{2}} = \delta_t u^{n-\frac{1}{2}} + r_1^{n-\frac{1}{2}} \tag{9}$$

and define the numerical scheme as

$$w^{n-\frac{1}{2}} = \Delta u^{n-\frac{1}{2}} - F(u^{n-1}) + f^{n-\frac{1}{2}} + r_2^{n-\frac{1}{2}}, \quad n \geq 1, \tag{10}$$

where

$$|r_1^{n-\frac{1}{2}}| \leq C_1 \delta t^2, \quad |r_2^{n-\frac{1}{2}}| \leq C_2 \delta t. \tag{11}$$

From (8), we have

$$w(\mathbf{x}, t_n) = \frac{1}{\Gamma(2-\alpha)} \int_0^{t_n} \frac{\partial v(\mathbf{x}, t)}{\partial t} \frac{dt}{(t_n-t)^{\alpha-1}}$$

using Lemma 2, we have

$$w^n = a_0 \left[b_0 v^n - \sum_{k=1}^{n-1} (b_{n-k-1} - b_{n-k}) v^k - b_{n-1} v^0 \right] + \mathcal{O}(\delta t^{3-\alpha}). \tag{12}$$

Now define the operator

$$\mathcal{P}(v^n, q) = \left[b_0 v^n - \sum_{k=1}^{n-1} (b_{n-k-1} - b_{n-k}) v^k - b_{n-1} q \right]$$

and using condition $v^0 = v(\mathbf{x}, 0) = \psi(\mathbf{x}) = \psi$, we have

$$w^{n-\frac{1}{2}} = a_0 \mathcal{P}(v^{n-\frac{1}{2}}, \psi) + r_3^{n-\frac{1}{2}} \tag{13}$$

where

$$|r_3^{n-\frac{1}{2}}| \leq C_3 \delta t^{3-\alpha} \tag{14}$$

Now substituting (9) into (13), we have

$$w^{n-\frac{1}{2}} = a_0 \mathcal{P}(\delta_t u^{n-\frac{1}{2}}, \psi) + a_0 \mathcal{P}(r_1^{n-\frac{1}{2}}, 0) + r_3^{n-\frac{1}{2}}, \tag{15}$$

now substituting above expression in (10), we have

$$\begin{aligned} a_0 \mathcal{P}(\delta_t u^{n-\frac{1}{2}}, \psi) + a_0 \mathcal{P}(r_1^{n-\frac{1}{2}}, 0) + r_3^{n-\frac{1}{2}} &= \Delta u^{n-\frac{1}{2}} - F(u^{n-1}) + f^{n-\frac{1}{2}} + r_2^{n-\frac{1}{2}} \\ a_0 \mathcal{P}(\delta_t u^{n-\frac{1}{2}}, \psi) &= \Delta u^{n-\frac{1}{2}} - F(u^{n-1}) + f^{n-\frac{1}{2}} + R^{n-\frac{1}{2}} \end{aligned} \tag{16}$$

where

$$\begin{aligned} R^{n-\frac{1}{2}} &= - \left\{ a_0 \mathcal{P}(r_1^{n-\frac{1}{2}}, 0) + r_3^{n-\frac{1}{2}} \right\} + r_2^{n-\frac{1}{2}} \\ |R^{n-\frac{1}{2}}| &\leq \left\{ a_0 \left[b_0 r_1^{n-\frac{1}{2}} + \sum_{k=1}^{n-1} (b_{n-k-1} - b_{n-k}) r_1^{k-\frac{1}{2}} \right] + r_3^{n-\frac{1}{2}} \right\} + r_2^{n-\frac{1}{2}} \\ &\leq \left\{ a_0 \left[b_0 C_1 \delta t^2 + \sum_{k=1}^{n-1} (b_{n-k-1} - b_{n-k}) C_1 \delta t^2 \right] + C_3 \delta t^{3-\alpha} \right\} + C_2 \delta t \\ &= \left\{ a_0 \left[b_0 C_1 \delta t^2 + (b_0 - b_{n-1}) C_1 \delta t^2 \right] + C_3 \delta t^{3-\alpha} \right\} + C_2 \delta t \\ &\leq \left\{ a_0 \left[2b_0 C_1 \delta t^2 \right] + C_3 \delta t^{3-\alpha} \right\} + C_2 \delta t \\ &= \left\{ \frac{1}{\delta t \Gamma(2-\alpha)} \left[2 \frac{\delta t^{2-\alpha}}{(2-\alpha)} C_1 \delta t^2 \right] + C_3 \delta t^{3-\alpha} \right\} + C_2 \delta t \\ &\leq C \delta t. \end{aligned}$$

where $C = \left\{ \frac{2C_1}{(2-\alpha)\Gamma(2-\alpha)} + C_2 + C_3 \right\}$.

Now omitting the truncation error term $R^{n-\frac{1}{2}}$, and approximating exact value u^n by its numerical approximation U^n , we have following discrete scheme

$$a_0 \mathcal{P}(\delta_t U^{n-\frac{1}{2}}, \psi) = \Delta U^{n-\frac{1}{2}} - F(U^{n-1}) + f^{n-\frac{1}{2}}, \quad 1 \leq n \leq N, \tag{17}$$

or equivalently we have

$$\mathcal{L}U^n = b \tag{18}$$

where \mathcal{L} is linear differential operator and b is function that contained contribution from previous time level and given as:

$$\begin{aligned} \mathcal{L}U^n &= a_0 \frac{b_0}{\delta t} U^n - \frac{1}{2} \Delta U^n \\ b &= a_0 \frac{b_0}{\delta t} U^{n-1} + \frac{1}{2} \Delta U^{n-1} + a_0 \sum_{k=1}^{n-1} (b_{n-k-1} - b_{n-k}) \delta t U^{k-\frac{1}{2}} \\ &\quad + a_0 b_{n-1} U_t^0 - F(U^{n-1}) + f^{n-\frac{1}{2}} \end{aligned}$$

2.1 Error analysis: convergence and stability

Now we discuss the convergence and stability of the time discrete scheme in L_2 norm.

Lemma 4 For any $G = \{G_1, G_2, \dots\}$, and q , we have

$$\sum_{n=1}^m \mathcal{P}(G_n, q) G_n \geq \frac{t_m^{1-\alpha}}{2} \delta t \sum_{n=1}^m G_n^2 - \frac{t_m^{2-\alpha}}{2(2-\alpha)} q^2$$

Proof See [38]. □

Lemma 5 (Discrete Gronwall Lemma) Assume that x_n is nonnegative sequence, and that the sequence y_n satisfies

$$\begin{cases} y_0 \leq \delta_0, \\ y_n \leq \delta_0 + \sum_{k=0}^{n-1} z_k + \sum_{k=0}^{n-1} x_k y_k \quad n \geq 1, \end{cases}$$

then y_n satisfies

$$\begin{cases} y_1 \leq \delta_0(1 + x_0) + z_0, \\ y_n \leq \delta_0 \prod_{k=0}^{n-1} (1 + x_k) + \sum_{k=0}^{n-2} z_k \prod_{s=k+1}^{n-1} (1 + x_s) + z_{n-1} \quad n \geq 2. \end{cases}$$

Moreover, if $\delta_0 \geq 0$ and $z_n \geq 0$ for $n \geq 0$, it follows

$$y_n \leq \left(\delta_0 + \sum_{k=0}^{n-1} z_k \right) \exp \left(\sum_{k=0}^{n-1} x_k \right), \quad n \geq 1.$$

Proof See [34]. □

Theorem 1 Let U^n and \tilde{U}^n be the exact and approximated solution of the (17) respectively, both belonging to H_0^1 . Then the time discrete scheme (17) is unconditionally stable and have the following inequality:

$$\|e^n\| \leq C \|\nabla e^0\|$$

where $e^n = U^n - \tilde{U}^n$.

Proof The error equation is

$$a_0 \left[b_0 \delta_t e^{n-\frac{1}{2}} - \sum_{k=1}^{n-1} (b_{n-k-1} - b_{n-k}) \delta_t e^{k-\frac{1}{2}} \right] = \Delta e^{n-\frac{1}{2}} - \left[F(U^{n-1}) - F(\tilde{U}^{n-1}) \right], \tag{19}$$

now multiplying above equation with by $\delta_t e^{n-\frac{1}{2}}$, and integrating over Ω , we have

$$\begin{aligned} & a_0 \left\{ b_0 \left(\delta_t e^{n-\frac{1}{2}}, \delta_t e^{n-\frac{1}{2}} \right) - \sum_{k=1}^{n-1} (b_{n-k-1} - b_{n-k}) \left(\delta_t e^{k-\frac{1}{2}}, \delta_t e^{n-\frac{1}{2}} \right) \right\} \\ & = \left(\Delta e^{n-\frac{1}{2}}, \delta_t e^{n-\frac{1}{2}} \right) - \left(\left[F(U^{n-1}) - F(\tilde{U}^{n-1}) \right], \delta_t e^{n-\frac{1}{2}} \right), \end{aligned} \tag{20}$$

now using the fact

$$\begin{aligned} \left(\Delta e^{n-\frac{1}{2}}, \delta_t e^{n-\frac{1}{2}} \right) & = - \left(\nabla e^{n-\frac{1}{2}}, \nabla \delta_t e^{n-\frac{1}{2}} \right) \\ & = - \int_{\Omega} \left(\frac{\nabla e^n + \nabla e^{n-1}}{2} \right) \left(\frac{\nabla e^n - \nabla e^{n-1}}{\delta t} \right) d\Omega \\ & = - \frac{1}{2\delta t} \int_{\Omega} \left[(\nabla e^n)^2 - \nabla e^{n-1} \right]^2 \\ & = - \frac{1}{2\delta t} \left(\|\nabla e^n\|^2 - \|\nabla e^{n-1}\|^2 \right), \end{aligned}$$

we have

$$\begin{aligned} & a_0 \left\{ b_0 \|\delta_t e^{n-\frac{1}{2}}\|^2 - \sum_{k=1}^{n-1} (b_{n-k-1} - b_{n-k}) \|\delta_t e^{k-\frac{1}{2}}\| \|\delta_t e^{n-\frac{1}{2}}\| \right\} \\ & \leq - \frac{1}{2\delta t} \left(\|\nabla e^n\|^2 - \|\nabla e^{n-1}\|^2 \right) - \left(\left[F(U^{n-1}) - F(\tilde{U}^{n-1}) \right], \delta_t e^{n-\frac{1}{2}} \right), \end{aligned} \tag{21}$$

now summing up both side of the above inequality from $n = 1$ to $n = m$, we have

$$\begin{aligned} & a_0 \sum_{n=1}^m \left\{ b_0 \|\delta_t e^{n-\frac{1}{2}}\|^2 - \sum_{k=1}^{n-1} (b_{n-k-1} - b_{n-k}) \|\delta_t e^{k-\frac{1}{2}}\| \|\delta_t e^{n-\frac{1}{2}}\| \right\} \\ & \leq - \frac{1}{2\delta t} \left(\|\nabla e^m\|^2 - \|\nabla e^0\|^2 \right) - \sum_{n=1}^m \left(\left[F(U^{n-1}) - F(\tilde{U}^{n-1}) \right], \delta_t e^{n-\frac{1}{2}} \right). \end{aligned} \tag{22}$$

Now since $F(u)$ satisfies Lipschitz condition with Lipschitz constant L , so we have

$$- \sum_{n=1}^m \left(\left[F(U^{n-1}) - F(\tilde{U}^{n-1}) \right], \delta_t e^{n-\frac{1}{2}} \right) \leq L \sum_{n=1}^m \left(|e^{n-1}|, |\delta_t e^{n-\frac{1}{2}}| \right),$$

also using inequality $|xy| \leq \frac{1}{2\theta}x^2 + \frac{\theta}{2}y^2$, together with $\theta = \frac{t_m^{1-\alpha}}{\Gamma(2-\alpha)}$, we have

$$\begin{aligned}
 & - \sum_{n=1}^m \left(\left[F(U^{n-1}) - F(\tilde{U}^{n-1}) \right], \delta_t e^{n-\frac{1}{2}} \right) \leq L^2 \frac{\Gamma(2-\alpha)}{2t_m^{1-\alpha}} \sum_{n=1}^m \|e^{n-1}\|^2 \\
 & + \frac{t_m^{1-\alpha}}{2\Gamma(2-\alpha)} \sum_{n=1}^m \|\delta_t e^{n-\frac{1}{2}}\|^2.
 \end{aligned}$$

Now using above relation together with Lemma 4, we have

$$\begin{aligned}
 a_0 \frac{t_m^{1-\alpha}}{2} \delta t \sum_{n=1}^m \|\delta_t e^{n-\frac{1}{2}}\|^2 & \leq -\frac{1}{2\delta t} \left(\|\nabla e^m\|^2 - \|\nabla e^0\|^2 \right) \\
 & + L^2 \frac{\Gamma(2-\alpha)}{2t_m^{1-\alpha}} \sum_{n=1}^m \|e^{n-1}\|^2 + \frac{t_m^{1-\alpha}}{2\Gamma(2-\alpha)} \sum_{n=1}^m \|\delta_t e^{n-\frac{1}{2}}\|^2.
 \end{aligned}$$

Now simplifying above relation and changing index from m to n , we have

$$\|\nabla e^n\|^2 \leq \|\nabla e^0\|^2 + L^2 \Gamma(2-\alpha) t_n^{\alpha-1} \delta t \sum_{j=0}^{n-1} \|e^j\|^2 \tag{23}$$

Finally, using Poincare inequality [7], $\|e^n\|^2 \leq C_\Omega^2 \|\nabla e^n\|^2$, we have

$$\|e^n\|^2 \leq C_\Omega^2 \|\nabla e^0\|^2 + L^2 C_\Omega^2 \Gamma(2-\alpha) t_n^{\alpha-1} \delta t \sum_{j=0}^{n-1} \|e^j\|^2. \tag{24}$$

The application of Discrete Gronwall Lemma 5, with parameters $z_k = 0$, $\delta_0 = C_\Omega^2 \|\nabla e^0\|^2$, $x_k = \delta t L^2 C_\Omega^2 \Gamma(2-\alpha) t_n^{\alpha-1}$, and $y_k = \|e^k\|^2$, we have

$$\begin{aligned}
 \|e^n\|^2 & \leq C_\Omega^2 \|\nabla e^0\|^2 \prod_{k=0}^{n-1} \left(1 + L^2 C_\Omega^2 \Gamma(2-\alpha) \delta t t_n^{\alpha-1} \right) \\
 & \leq C_\Omega^2 \|\nabla e^0\|^2 \exp \left(\sum_{k=0}^{n-1} \left(L^2 C_\Omega^2 \Gamma(2-\alpha) \delta t t_n^{\alpha-1} \right) \right) \\
 & \leq C_\Omega^2 \exp \left(L^2 C_\Omega^2 \Gamma(2-\alpha) n \delta t t_n^{\alpha-1} \right) \|\nabla e^0\|^2 \\
 & = C_\Omega^2 \exp \left(L^2 C_\Omega^2 \Gamma(2-\alpha) t_n^\alpha \right) \|\nabla e^0\|^2 \\
 & \leq C_\Omega^2 \exp \left(L^2 C_\Omega^2 \Gamma(2-\alpha) T^2 \right) \|\nabla e^0\|^2
 \end{aligned}$$

Therefore we have

$$\|e^n\| \leq C \|\nabla e^0\|,$$

where $C = C_\Omega \sqrt{\exp(L^2 C_\Omega^2 \Gamma(2-\alpha) T^2)}$. □

Theorem 2 *Let u^n and U^n be the solution of (16) and (17), respectively, such that both belonging to H_0^1 . Then time semi-discrete scheme (17) is convergent with convergence order $O(\delta t)$.*

Proof Let us define $\mathcal{E}^n = u^n - U^n$ for $n \geq 1$, together with $\mathcal{E}^0 = 0$. Now subtracting (17) from (16), we have

$$a_0 \mathcal{P}(\delta_t \mathcal{E}^{n-\frac{1}{2}}, 0) = \Delta \mathcal{E}^{n-\frac{1}{2}} - \left[F(u^{n-1}) - F(U^{n-1}) \right] + R^{n-\frac{1}{2}}, \tag{25}$$

multiplying above equation by $\delta_t \mathcal{E}^{n-\frac{1}{2}}$, and integrating over Ω , we get

$$\begin{aligned} & a_0 \left\{ b_0 \|\delta_t \mathcal{E}^{n-\frac{1}{2}}\| - \sum_{k=1}^{n-1} (b_{n-k-1} - b_{n-k}) \|\delta_t \mathcal{E}^{k-\frac{1}{2}}\| \right\} \|\delta_t \mathcal{E}^{n-\frac{1}{2}}\| \\ &= -\frac{1}{2\delta t} \left(\|\nabla \mathcal{E}^n\|^2 - \|\nabla \mathcal{E}^{n-1}\|^2 \right) \\ & \quad - \left(\left[F(u^{n-1}) - F(U^{n-1}) \right], \delta_t \mathcal{E}^{n-\frac{1}{2}} \right) + \left(R^{n-\frac{1}{2}}, \delta_t \mathcal{E}^{n-\frac{1}{2}} \right) \end{aligned}$$

Now summing the above relation from $n = 1$ to m , we have

$$\begin{aligned} & a_0 \sum_{n=1}^m \left\{ b_0 \|\delta_t \mathcal{E}^{n-\frac{1}{2}}\| - \sum_{k=1}^{n-1} (b_{n-k-1} - b_{n-k}) \|\delta_t \mathcal{E}^{k-\frac{1}{2}}\| \right\} \|\delta_t \mathcal{E}^{n-\frac{1}{2}}\| \\ & \leq -\frac{1}{2\delta t} \left(\|\nabla \mathcal{E}^m\|^2 - \|\nabla \mathcal{E}^0\|^2 \right) \\ & \quad - \sum_{n=1}^m \left(\left[F(u^{n-1}) - F(U^{n-1}) \right], \delta_t \mathcal{E}^{n-\frac{1}{2}} \right) + \sum_{n=1}^m \|R^{n-\frac{1}{2}}\| \|\delta_t \mathcal{E}^{n-\frac{1}{2}}\|, \end{aligned}$$

now application of Lemma 4, yields

$$\begin{aligned} a_0 \frac{t_m^{1-\alpha}}{2} \delta t \sum_{n=1}^m \|\delta_t \mathcal{E}^{n-\frac{1}{2}}\|^2 + \frac{1}{2\delta t} \|\nabla \mathcal{E}^m\|^2 & \leq - \sum_{n=1}^m \left(\left[F(u^{n-1}) - F(U^{n-1}) \right], \delta_t \mathcal{E}^{n-\frac{1}{2}} \right) \\ & \quad + \sum_{n=1}^m \|R^{n-\frac{1}{2}}\| \|\delta_t \mathcal{E}^{n-\frac{1}{2}}\|. \end{aligned} \tag{26}$$

Using inequality $|xy| \leq \frac{1}{2\theta} x^2 + \frac{\theta}{2} y^2$, together with $\theta = \frac{t_m^{1-\alpha}}{2\Gamma(2-\alpha)}$, we have

$$\begin{aligned} - \sum_{n=1}^m \left(\left[F(u^{n-1}) - F(U^{n-1}) \right], \delta_t \mathcal{E}^{n-\frac{1}{2}} \right) & \leq L^2 \frac{\Gamma(2-\alpha)}{t_m^{1-\alpha}} \sum_{n=1}^m \|\mathcal{E}^{n-1}\|^2 \\ & \quad + \frac{t_m^{1-\alpha}}{4\Gamma(2-\alpha)} \sum_{n=1}^m \|\delta_t \mathcal{E}^{n-\frac{1}{2}}\|^2 \\ \sum_{n=1}^m \|R^{n-\frac{1}{2}}\| \|\delta_t \mathcal{E}^{n-\frac{1}{2}}\| & \leq \frac{\Gamma(2-\alpha)}{t_m^{1-\alpha}} \sum_{n=1}^m \|R^{n-\frac{1}{2}}\|^2 \\ & \quad + \frac{t_m^{1-\alpha}}{4\Gamma(2-\alpha)} \sum_{n=1}^m \|\delta_t \mathcal{E}^{n-\frac{1}{2}}\|^2. \end{aligned}$$

Using above relation into (26), we have

$$\begin{aligned} \frac{t_m^{1-\alpha}}{2\Gamma(2-\alpha)} \sum_{n=1}^m \|\delta_t \mathcal{E}^{n-\frac{1}{2}}\|^2 + \frac{1}{2\delta t} \|\nabla \mathcal{E}^m\|^2 &\leq L^2 \frac{\Gamma(2-\alpha)}{t_m^{1-\alpha}} \sum_{n=1}^m \|\mathcal{E}^{n-1}\|^2 \\ &+ \frac{t_m^{1-\alpha}}{4\Gamma(2-\alpha)} \sum_{n=1}^m \|\delta_t \mathcal{E}^{n-\frac{1}{2}}\|^2 \\ &+ \frac{\Gamma(2-\alpha)}{t_m^{1-\alpha}} \sum_{n=1}^m \|R^{n-\frac{1}{2}}\|^2 \\ &+ \frac{t_m^{1-\alpha}}{4\Gamma(2-\alpha)} \sum_{n=1}^m \|\delta_t \mathcal{E}^{n-\frac{1}{2}}\|^2, \end{aligned}$$

changing index from m to n , multiplying both sides by $2\delta t$, and after simplification we get

$$\begin{aligned} \|\nabla \mathcal{E}^n\|^2 &\leq 2\delta t L^2 \Gamma(2-\alpha) t_n^{\alpha-1} \sum_{j=0}^{n-1} \|\mathcal{E}^j\|^2 + 2\delta t \Gamma(2-\alpha) t_n^{\alpha-1} \sum_{j=1}^n \|R^{j-\frac{1}{2}}\|^2 \\ &\leq 2\delta t L^2 \Gamma(2-\alpha) t_n^{\alpha-1} \sum_{j=0}^{n-1} \|\mathcal{E}^j\|^2 + 2n\delta t \Gamma(2-\alpha) t_n^{\alpha-1} \max_{1 \leq j \leq n} \|R^{j-\frac{1}{2}}\|^2. \end{aligned}$$

Now using Poincare inequality [7], we have

$$\|\mathcal{E}^n\|^2 \leq C_\Omega^2 \delta t L^2 \Gamma(2-\alpha) t_n^{\alpha-1} \sum_{j=0}^{n-1} \|\mathcal{E}^j\|^2 + C_\Omega^2 \Gamma(2-\alpha) T C^2 \delta t^2, \tag{27}$$

now using Lemma 5, with parameters $z_k = 0$, $\delta_0 = C_\Omega^2 C^2 T \Gamma(2-\alpha) \delta t^2$, $x_k = \delta t L^2 C_\Omega^2 \Gamma(2-\alpha) t_n^{\alpha-1}$, and $y_k = \|\mathcal{E}^k\|^2$ yields:

$$\begin{aligned} \|\mathcal{E}^n\|^2 &\leq T C^2 C_\Omega^2 \Gamma(2-\alpha) \delta t^2 \exp\left(\sum_{k=0}^{n-1} (L^2 C_\Omega^2 \Gamma(2-\alpha) \delta t t_n^{\alpha-1})\right) \\ &\leq T C^2 C_\Omega^2 \Gamma(2-\alpha) \delta t^2 \exp\left(L^2 C_\Omega^2 \Gamma(2-\alpha) n \delta t t_n^{\alpha-1}\right) \\ &= T C^2 C_\Omega^2 \Gamma(2-\alpha) \delta t^2 \exp\left(L^2 C_\Omega^2 \Gamma(2-\alpha) t_n^\alpha\right) \\ &\leq T C^2 C_\Omega^2 \Gamma(2-\alpha) \delta t^2 \exp\left(L^2 C_\Omega^2 \Gamma(2-\alpha) T^2\right) \\ &\leq C(T, \alpha, C_\Omega) \delta t^2. \end{aligned}$$

Therefore, we have

$$\|\mathcal{E}^n\| \leq C'(T, \alpha, C_\Omega) \delta t,$$

which completes the proof. □

3 Spatial discretization by the local collocation method

In local collocation method, the computational domain Ω , containing M collocation points, is partitioned into M overlapping sub domains Ω_i , such that $\bigcup_{i=1}^M \Omega_i = \Omega$. For each $\mathbf{x}_k^{[i]} \in \Omega_i$, the influence points of $\mathbf{x}_k^{[i]}$ are $\{\mathbf{x}_1^{[i]}, \mathbf{x}_2^{[i]}, \mathbf{x}_3^{[i]}, \dots, \mathbf{x}_{m_i}^{[i]}\}$ are m_i closest points of $\mathbf{x}_k^{[i]}$ in sub domain Ω_i .

The numerical approximation of $u(\mathbf{x}, t_n)$ in local interpolation form can be given as

$$\hat{u}(\mathbf{x}, t_n) = \sum_{j=1}^{m_i} \lambda_j \phi \left(\|\mathbf{x} - \mathbf{x}_j^{[i]}\| \right) + \sum_{j=1}^l \gamma_j p_j(\mathbf{x}), \tag{28}$$

where $\{\lambda_j\}$ and $\{\gamma_j\}$ are unknown coefficients at n th time level, ϕ is considered radial basis function, $\|\cdot\|$ is the Euclidean norm, and $\{p_j(x)\}_{j=1}^l$ denotes basis for the $l = \binom{m-1+d}{m-1}$ dimensional linear space of d -variate polynomials of total degree $\leq m - 1$. The interpolation condition on sub-domain Ω_i

$$\hat{u} \left(\mathbf{x}_k^{[i]}, t_n \right) = u \left(\mathbf{x}_k^{[i]}, t_n \right), \quad \forall 1 \leq k \leq m_i, \tag{29}$$

is supported with extra l regularization conditions

$$\sum_{j=1}^{m_i} \lambda_j p_k \left(\mathbf{x}_j^{[i]} \right) = 0 \quad \forall 1 \leq k \leq l. \tag{30}$$

Imposing conditions (29)–(30) on $\hat{u}(\mathbf{x}, t_n)$, at each stencil, we obtain following linear system

$$\begin{bmatrix} \Phi & P \\ P^t & O \end{bmatrix} \begin{bmatrix} \lambda \\ \gamma \end{bmatrix} = \begin{bmatrix} u |_{\Omega_i} \\ O \end{bmatrix} \tag{31}$$

where $\Phi := \left[\phi \|\mathbf{x}_j^{[i]} - \mathbf{x}_k^{[i]}\| \right]_{1 \leq j, k \leq m_i}$, $P := \left[p_k(\mathbf{x}_j^{[i]}) \right]_{1 \leq j \leq m_i, 1 \leq k \leq l}$.

The above system can be written in matrix form as

$$A_{\Omega_i} = A_{\Omega_i}^{-1} U_{\Omega_i}^n, \tag{32}$$

where $A_{\Omega_i} = [\lambda_1, \dots, \lambda_{m_i}, \gamma_1, \dots, \gamma_l]^T$, $U_{\Omega_i}^n = \left[u(\mathbf{x}_1^{[i]}, t_n), \dots, u(\mathbf{x}_{m_i}^{[i]}, t_n), 0, \dots, 0 \right]^T$, and A_{Ω_i} is coefficient matrix of the system (31).

Suppose ϕ is a conditionally positive definite function of order m on \mathbb{R}^d and the points $\Omega_i = \{x_1, x_2, \dots, x_{m_i}\}$ form $(m - 1)$ unisolvent set of centers. Then the system (31) is uniquely solvable.

For a linear differential operator \mathcal{D} , at each stencil $\mathbf{x}_k^{[i]} \in \Omega_i$, we have approximation for $\mathcal{D}u(\mathbf{x}, t_n)$ as;

$$\begin{aligned} \mathcal{D}\hat{u}(\mathbf{x}_k^{[i]}, t_n) &= \sum_{j=1}^{m_i} \lambda_j \mathcal{D}\phi(\|\mathbf{x}_k^{[i]} - \mathbf{x}_j^{[i]}\|) + \sum_{j=1}^l \gamma_j \mathcal{D}p_j(\mathbf{x}_k^{[i]}), \\ &= [\mathcal{D}\phi(\|\mathbf{x}_k^{[i]} - \mathbf{x}_1^{[i]}\|), \dots, \mathcal{D}\phi(\|\mathbf{x}_k^{[i]} - \mathbf{x}_{m_i}^{[i]}\|), \mathcal{D}p_1(\mathbf{x}_k^{[i]}), \dots, \mathcal{D}p_l(\mathbf{x}_k^{[i]})] \Lambda_{\Omega_i} \\ &= \mathcal{D}\Psi_{\Omega_i} A_{\Omega_i}^{-1} U_{\Omega_i}^n, \end{aligned} \tag{33}$$

where $\Psi_{\Omega_i} = [\phi(\|\mathbf{x}_k^{[i]} - \mathbf{x}_1^{[i]}\|), \dots, \phi(\|\mathbf{x}_k^{[i]} - \mathbf{x}_{m_i}^{[i]}\|), p_1(\mathbf{x}_k^{[i]}), \dots, p_l(\mathbf{x}_k^{[i]})]$. For each k , the local operator $\mathcal{D}\Psi_{\Omega_i} A_{\Omega_i}^{-1}$ is a $1 \times m_i$ row vector.

Now for each collocation points $\mathbf{x}_i \in \Omega$, applying the local collocation method described through (33) to the linear operator \mathcal{L} defined in (18), we have

$$\mathcal{L}\Psi_{\Omega_i} A_{\Omega_i}^{-1} U_{\Omega_i}^n = b_i, \mathbf{x}_i \in \Omega. \tag{34}$$

For each arbitrary i , the $\mathcal{L}\Psi_{\Omega_i} A_{\Omega_i}^{-1}$ is a $1 \times m_i$ row vector, that going to store in $M \times M$ matrix, by filling extra spaces by zeros. Thus, we have following linear system

$$\mathbf{L}\mathbf{U}^n = \mathbf{b}. \tag{35}$$

The resulting system is sparse having only m_i nonzero entries in each rows, and hence can be calculate efficiently.

4 Numerical simulation and discussion

In this section, we present several numerical experiments to illustrate the efficiency and accuracy of proposed method. The accuracy of the proposed method is measured against two different error measurement viz maximum absolute error L_∞ , and root mean square error L_{rms} , defined by using following definition

$$L_\infty = \max_{1 \leq i \leq M} |u(\mathbf{x}_i, T) - U(\mathbf{x}_i, T)|, \quad L_{rms} = \sqrt{\frac{1}{M} \sum_{i=1}^M |u(\mathbf{x}_i, T) - U(\mathbf{x}_i, T)|^2},$$

where $u(\mathbf{x}_i, T)$ and $U(\mathbf{x}_i, T)$ represent analytical and numerical solution and M is number of collocation points inside the domain Ω .

Since accuracy of RBF-based methods is highly influenced by shape parameter ϵ , choosing an optimal value of ϵ is itself a crucial task. To overcome this complication, we will use the second-order thin plate spline $r^{2\beta} \ln(r)$, with $\beta = 2$, in our all numerical experiments; however, a higher-order function can be used for better accuracy. To show the efficiency of meshless nature of the proposed method, some irregular

domain is also considered (see Fig. 1). The boundary Γ_k of irregular domain Ω_k , for $k = 1, 2$ is defined by the parametric equations

$$\Gamma_1 = \left\{ (r \cos(\theta), r \sin(\theta)) : r = \frac{1}{64} [81 - 9 \cos(8\theta)] \right\}$$

$$\Gamma_2 = \left\{ (r \cos(\theta), r \sin(\theta)) : r = \frac{1}{9} [17 - 8 \cos(3\theta)] \right\}.$$

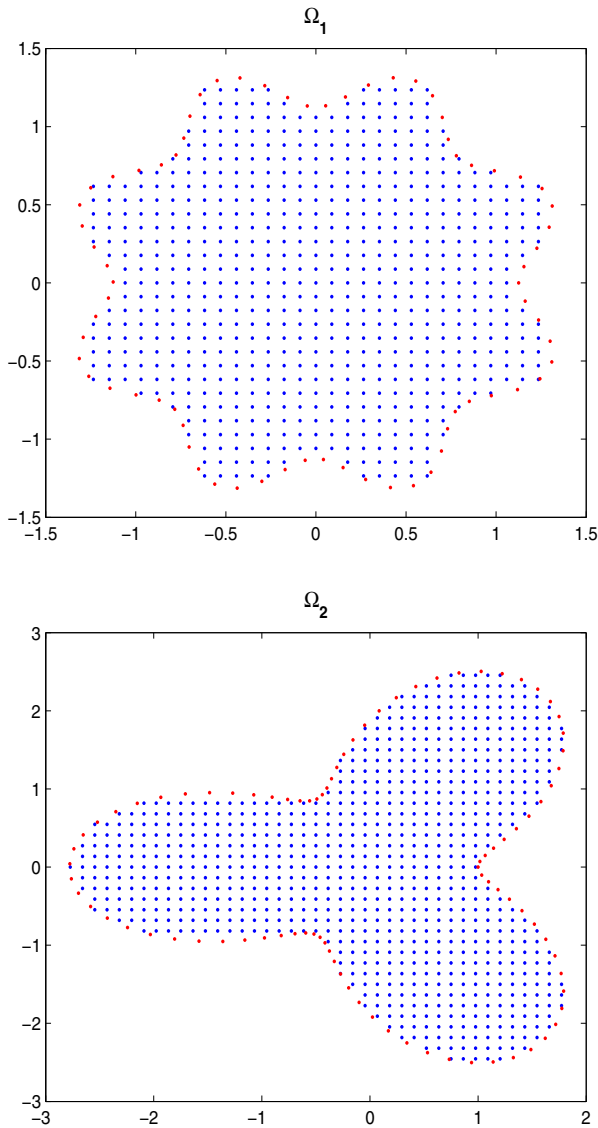


Fig. 1 The considered irregular domains for two-dimensional test problem

Now we will deal with some numerical experiments for validating our proposed method. We consider two different cases as

Case I $F(u(\mathbf{x}, t)) = \sin(u(\mathbf{x}, t))$, Sine Gordon

Case II $F(u(\mathbf{x}, t)) = u(\mathbf{x}, t)^3$, Klein Gordon.

Example 1 Consider following test problem

$${}^c \mathcal{D}_t^\alpha u(x, y, t) = \Delta u(x, y, t) - F(u(x, y, t)) + f(x, y, t).$$

The initial conditions and boundary conditions are extracted from the analytic solutions

$$u(x, y, t) = t^2 \sin(x + y).$$

The linear source terms read $f(x, y, t) = \left(\frac{2t^{2-\alpha}}{\Gamma(3-\alpha)} + 2t^2\right) \sin(x+y) + F(u(x, y, t))$.

First, we deal for case I, the Sine-Gordon equation. We solve the present problem in the computation domain $[-1, 1]^2$, with 21×21 uniform points for different values of α and δt . The computational results for thin plate spline $r^4 \ln r$ with $m = 5$ are reported in Table 1. In Fig. 2, we plotted the numerical solution and absolute error at $T = 1$.

We also extended the same numerical experiment setup on the irregular domain Ω_1 and Ω_2 . The numerical results for computational domain Ω_1 with 645 internal points and 70 boundary points that is total collocation points $M = 715$ and $m = 9$ are reported in Table 2. Finally, in Table 3, we did same numerical experiment on experimental domain Ω_2 . In this numerical experiment, we considered 798 internal points and 90 boundary points.

From all these tables, we can conclude that both errors are decreasing as δt decreases and experimental convergence in time is approximate to $\mathcal{O}(\delta t)$. Finally, we also compared our method with collocation method presented by Dehghan et al. [12] and comparison results are reported in Table 4. From the table, we can observe that method presented in [12] is accurate up to three decimal place using 320 temporal

Table 1 The value of errors with different values of α and δt on domain $[-1, 1]^2$ at time $T = 1.0$ s for Example 1 with case I

δt	$\alpha = 1.25$			$\alpha = 1.75$			Rate	cpu (s)	
	L_∞	Rate	L_{rms}	L_∞	Rate	L_{rms}			
1/10	6.1465e-03	–	2.9672e-03	–	7.4024e-03	–	3.5206e-03	–	0.371
1/20	3.1227e-03	0.99	1.5077e-03	0.99	3.8275e-03	0.95	1.8176e-03	0.95	0.403
1/40	1.6145e-03	0.98	7.8001e-04	0.98	1.9820e-03	0.95	9.4142e-04	0.95	0.453
1/80	8.6143e-04	0.96	4.1637e-04	0.96	1.0446e-03	0.93	4.9710e-04	0.93	0.673
1/160	4.8547e-04	0.92	2.3457e-04	0.91	5.7332e-04	0.90	2.7352e-04	0.90	1.197

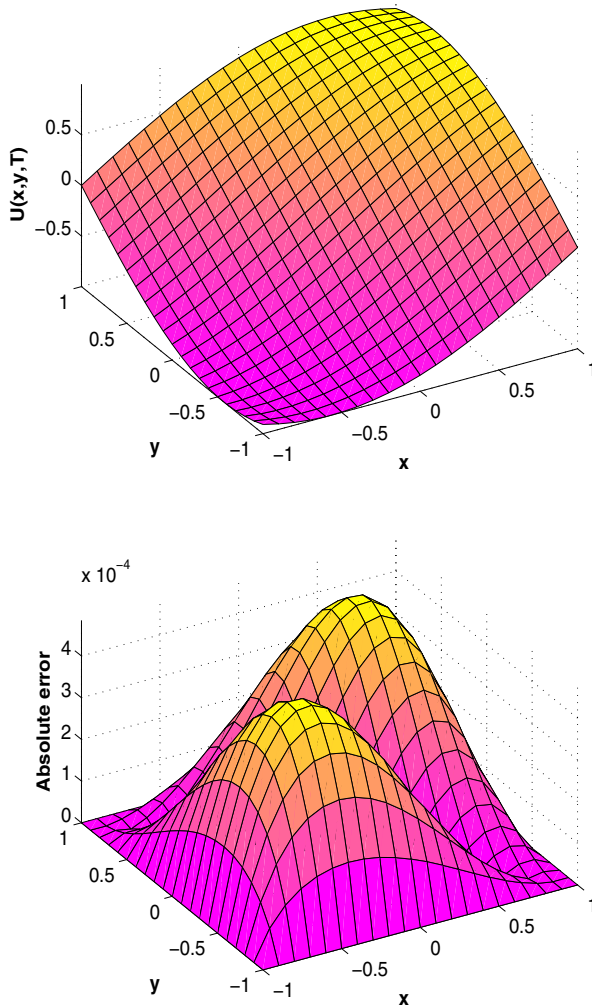


Fig. 2 Numerical solution and absolute error at $T = 1$ for $\alpha = 1.25$, and $N = 441$ on domain $[-1, 1]^2$ for Example 1 with case I

points, although the proposed method reached better accuracy only in 160 temporal points.

Now we extended our numerical experiments for same test problem with case II, the Klein Gordon equations. We did same numerical experiments on domain $[0, 1]^2$ with 21×21 and two different errors for different values of α are reported in Table 5. Finally, In Fig. 3, we plotted absolute error for different values of time and α for test case II.

Example 2 Consider following test problem

$${}_0^c \mathcal{D}_t^\alpha u(x, y, t) = \Delta u(x, y, t) - F(u(x, y, t)) + f(x, y, t).$$

Table 2 The value of errors with different values of α and δt on domain Ω_1 at time $T = 1.0$ s for Example 1 with case I

δt	$\alpha = 1.25$				$\alpha = 1.75$				cpu (s)
	L_∞	Rate	L_{rms}	Rate	L_∞	Rate	L_{rms}	Rate	
1/10	7.2699e-03	—	3.6303e-03	—	8.7526e-03	—	4.3112e-03	—	0.749
1/20	3.4584e-03	1.07	1.7233e-03	1.07	4.3212e-03	1.02	2.1168e-03	1.02	0.827
1/40	1.5570e-03	1.15	7.7202e-04	1.15	2.0337e-03	1.10	9.8877e-04	1.10	0.999
1/80	6.0737e-04	1.37	2.9714e-04	1.37	8.7234e-04	1.20	4.1763e-04	1.20	1.363
1/160	1.4006e-04	2.11	6.3810e-05	2.11	2.8881e-04	1.50	1.3224e-04	1.50	2.395

Table 3 The value of errors with different values of α and δt on domain Ω_2 at time $T = 1.0$ s for Example 1 with case I

δt	$\alpha = 1.25$				$\alpha = 1.75$				cpu (s)
	L_∞	Rate	L_{rms}	Rate	L_∞	Rate	L_{rms}	Rate	
1/10	1.5694e-02	—	7.4645e-03	—	1.5537e-02	—	7.4946e-03	—	0.724
1/20	7.2768e-03	1.10	3.4700e-03	1.10	7.3858e-03	1.07	3.5663e-03	1.07	0.810
1/40	3.0532e-03	1.25	1.4708e-03	1.24	3.2821e-03	1.16	1.5922e-03	1.17	0.854
1/80	9.3850e-04	1.70	4.8604e-04	1.60	1.2236e-03	1.42	6.1196e-04	1.37	0.892
1/160	3.1719e-04	1.50	1.6619e-04	1.55	6.3644e-04	1.04	1.7952e-04	1.40	0.937

Table 4 Absolute error comparison of proposed method with Dehghan et al. [12] for Example 1 with case I

δt	$\alpha = 1.25$		$\alpha = 1.75$	
	Dehghan et al. [12]	Present method	Dehghan et al. [12]	Present method
1/10	1.6803e-02	6.4470e-03	1.1295e-02	7.6510e-03
1/20	8.4912e-03	3.4316e-03	4.8061e-03	4.0967e-03
1/40	4.2901e-03	1.9274e-03	2.2178e-03	2.2614e-03
1/80	2.1780e-03	1.1757e-03	1.7179e-03	1.3294e-03
1/160	1.6190e-03	7.9985e-04	1.4745e-03	8.6004e-04
1/320	1.4288e-03	6.1192e-04	1.3831e-03	6.2466e-04

Table 5 The value of errors with different values of α and δt on domain $[0, 1]^2$ at time $T = 1.0$ s for Example 1 with case II

δt	$\alpha = 1.3$				$\alpha = 1.7$				cpu (s)
	L_∞	Rate	L_{rms}	Rate	L_∞	Rate	L_{rms}	Rate	
1/10	9.7153e-03	—	4.8882e-03	—	7.7454e-03	—	3.8907e-03	—	0.392
1/20	4.9045e-03	0.98	2.4684e-03	0.98	3.8178e-03	1.02	1.9160e-03	1.02	0.405
1/40	2.4666e-03	0.99	1.2418e-03	0.99	1.9000e-03	1.00	9.5361e-04	1.00	0.480
1/80	1.2445e-03	0.99	6.2682e-04	0.99	9.5560e-04	1.00	4.8010e-04	1.00	0.694
1/160	6.3315e-04	0.97	3.1921e-04	0.97	4.8700e-04	1.01	2.4525e-04	1.01	1.302

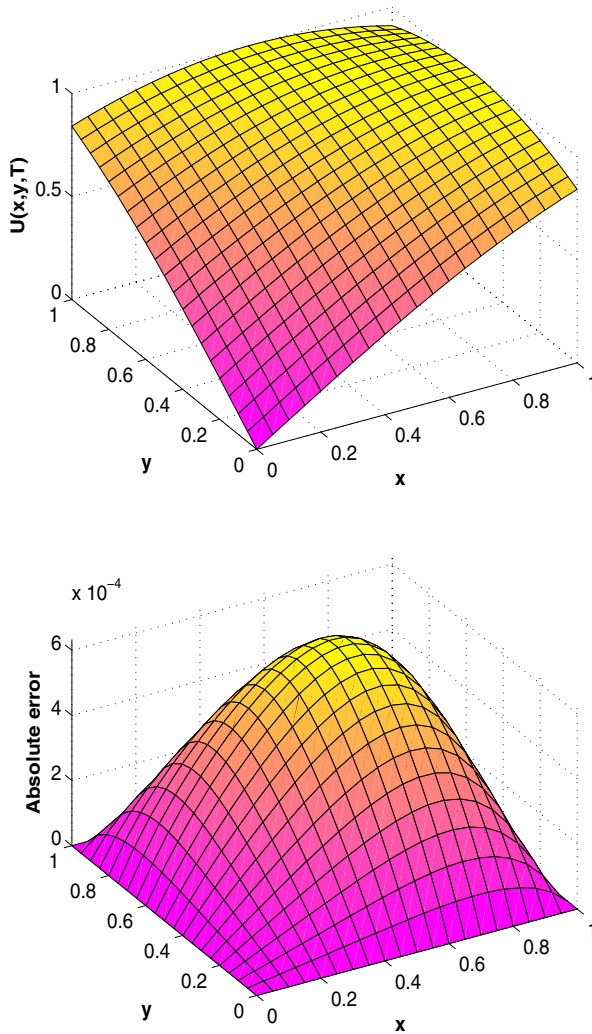


Fig. 3 Numerical solution and absolute error at $T = 1$ for $\alpha = 1.3$, for Example 1 and test case II

Table 6 The value of errors with different values of α and δt on domain $[0, 1]^2$ at time $T = 1.0$ s for Example 2 with case I

δt	$\alpha = 1.4$			$\alpha = 1.8$			Rate	cpu (s)	
	L_∞	Rate	L_{rms}	Rate	L_∞	Rate			
1/5	7.9545e-03	—	4.0107e-03	—	2.7225e-02	—	1.3681e-02	—	2.208
1/10	3.2422e-03	1.21	1.6389e-03	1.21	1.2445e-02	1.12	6.2551e-03	1.12	2.213
1/20	1.4002e-03	1.21	7.0898e-04	1.21	5.6499e-03	1.13	2.8399e-03	1.13	2.956
1/40	6.5482e-04	1.10	3.3179e-04	1.10	2.5781e-03	1.13	1.2960e-03	1.13	3.372
1/80	3.4063e-04	1.00	1.7252e-04	1.00	1.1987e-03	1.11	6.0258e-04	1.11	5.265

The initial conditions and boundary conditions are extracted from the analytic solutions

$$u(x, y, t) = \cos(\pi x) \cos(\pi y) t^{3+\alpha}.$$

The source terms is $f(x, y, t) = \left(\frac{\Gamma(4+\alpha)}{6} t^3 + 2\pi^2 t^{3+\alpha} \right) \cos(\pi x) \cos(\pi y) + F(u(x, y, t))$.

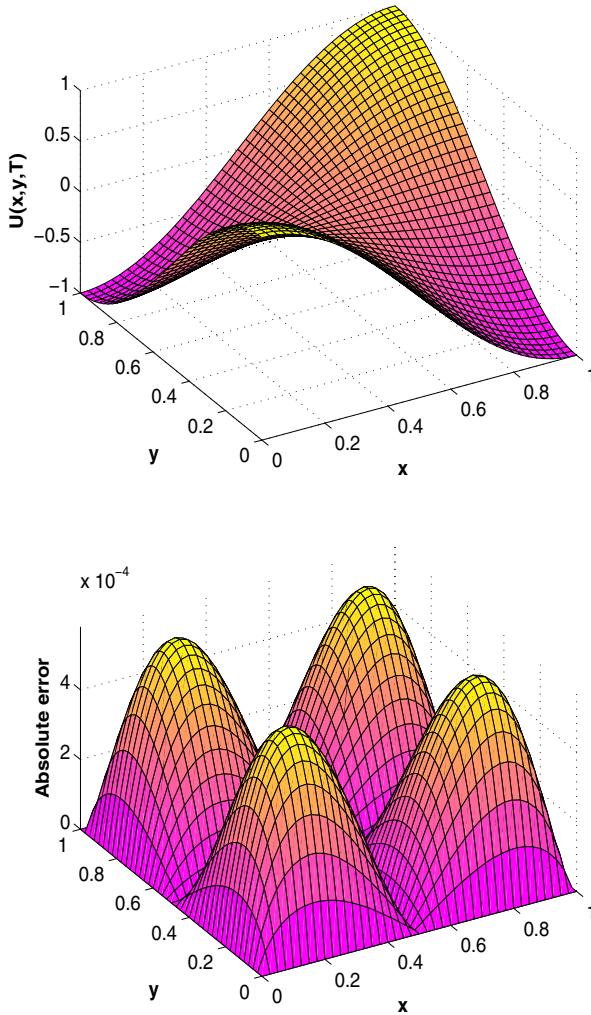


Fig. 4 Numerical solution and absolute error for $\alpha = 1.8$, at $T = 1$ s on domain $[0, 1]^2$ for Example 2 with case I

We solve the present problem in the computation domain $[0, 1]^2$, with 41×41 uniform points for different values of α and δt . The computational results with $m = 5$ are reported in Table 6.

The graph of numerical approximation of the solution and absolute error is plotted in Fig. 4 respectively. From Table 6, we can observe that for this test problem, also experimental convergence in time achieved is approximate to $\mathcal{O}(\delta t)$.

We are now extended our experiment to solve case II, and the experimental data are reported in Table 7. From the table, we observe the convergence achieved in time is approximate to $\mathcal{O}(\delta t)$. Finally, in Fig. 5, we plotted absolute errors at different values of α .

Example 3 Consider following test problem

$${}^c_0\mathcal{D}_t^\alpha u(x, y, t) = \Delta u(x, y, t) - F(u(x, y, t)) + f(x, y, t).$$

The initial conditions and boundary conditions are extracted from the analytic solutions

$$u(x, y, t) = t^2 e^{\frac{-(x-0.5)^2-(y-0.5)^2}{\beta}}.$$

The source terms is $f(x, y, t) = \left(\frac{2t^{2-\alpha}}{\Gamma(3-\alpha)} + t^2 \frac{4}{\beta} - t^2 \frac{4(x-0.5)^2}{\beta^2} - t^2 \frac{4(y-0.5)^2}{\beta^2} \right) e^{\frac{-(x-0.5)^2-(y-0.5)^2}{\beta}} + F(u(x, y, t)).$

This example is adopted from Dehghan et al. [8]. In [8], consider this example to validate the element-free Galerkin method for numerical solution of 2D fractional Tricomi-type equation. The proposed problem is solved in computational domain

Table 7 The value of errors with different values of α and δt on domain $[0, 1]^2$ at time $T = 1.0$ s for Example 2 with case II

δt	$\alpha = 1.25$			$\alpha = 1.75$			Rate	cpu (s)	
	L_∞	Rate	L_{rms}	Rate	L_∞	Rate			L_{rms}
1/5	5.6468e-03	—	2.6135e-03	—	2.2188e-02	—	1.1044e-02	—	2.050
1/10	2.8517e-03	0.99	1.2614e-03	1.05	1.0013e-02	1.15	4.9448e-03	1.16	2.164
1/20	1.4010e-03	1.02	6.0786e-04	1.05	4.4255e-03	1.18	2.1738e-03	1.19	2.585
1/40	7.0931e-04	0.98	3.0723e-04	0.98	1.9704e-03	1.17	9.6366e-04	1.17	3.274
1/80	3.8371e-04	0.89	1.6875e-04	0.89	9.0380e-04	1.12	4.4044e-04	1.13	4.948

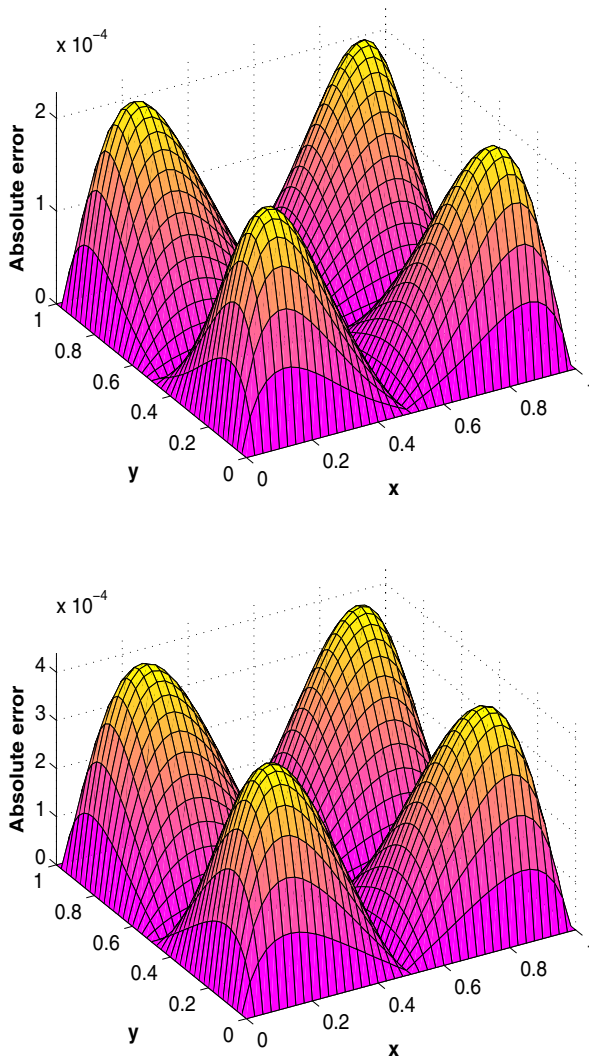


Fig. 5 Absolute error at time $T = 1$ s for different values of $\alpha = 1.25$ and $\alpha = 1.75$, on domain $[0, 1]^2$ for Example 2 with case II

$[0, 1]^2$, with 55×55 spatial points for different values of α . The different error at time $T = 1$ s with $\beta = 0.1$ is reported in Tables 8 and 9, for Sine Gordon and Klein Gordon equations respectively. From the table, we observe the convergence achieved in time is approximate to $\mathcal{O}(\delta t)$. Finally, in Fig. 6, we present the graphs

Table 8 The value of errors with different values of α and δt on domain $[0, 1]^2$ at time $T = 1.0$ s for Example 3 with case I

δt	$\alpha = 1.5$				$\alpha = 1.8$				cpu (s)
	L_∞	Rate	L_{rms}	Rate	L_∞	Rate	L_{rms}	Rate	
1/5	6.2323e-03	—	3.1311e-03	—	6.8385e-03	—	3.4227e-03	—	5.919
1/10	2.8527e-03	1.12	1.4828e-03	1.07	3.2588e-03	1.06	1.6780e-03	1.03	8.934
1/20	1.1899e-03	1.26	6.7153e-04	1.14	1.4219e-03	1.19	7.8225e-04	1.10	9.086
1/40	4.9328e-04	1.27	2.7574e-04	1.28	5.7392e-04	1.30	3.3168e-04	1.23	15.718
1/80	2.6525e-04	0.91	1.1081e-04	1.31	2.9353e-04	0.97	1.2838e-04	1.36	16.455

of approximate solution and absolute error using the proposed method for $\alpha = 1.8$, $\delta t = 0.001$, and $\beta = 0.005$ for 80×80 spatial points at time $T = 1$ s.

5 Conclusion

In this work, we have employed the radial basis function-based meshless local collocation method for the numerical solution of time fractional nonlinear diffusion wave equation. Basically we solve two family of equations sine Gordon and Klein Gordon equation. The time semi-discretization was done by finite difference method and spatial discretization was done by meshless method. To overcome the stability issue due to shape parameter, the thin plate spline is used as basis of the collocation method. The numerical experiments for different values of α are carried out. Numerical methods are employed on both regular and irregular domain. Numerical results show that the computation order of convergence in time is close to theoretical order.

Table 9 The value of errors with different values of α and δt on domain $[0, 1]^2$ at time $T = 1.0$ s for Example 3 with case II

δt	$\alpha = 1.5$				$\alpha = 1.8$				cpu (s)
	L_∞	Rate	L_{rms}	Rate	L_∞	Rate	L_{rms}	Rate	
1/5	8.6115e-03	—	3.1452e-03	—	7.6310e-03	—	2.7067e-03	—	6.623
1/10	4.1832e-03	1.04	1.5274e-03	1.04	3.5135e-03	1.11	1.2286e-03	1.13	6.985
1/20	1.8638e-03	1.16	6.9260e-04	1.14	1.4799e-03	1.24	5.2310e-04	1.23	7.934
1/40	6.9862e-04	1.41	2.8260e-04	1.29	4.9360e-04	1.58	1.9854e-04	1.39	10.608
1/80	2.2121e-04	1.65	1.0846e-04	1.38	2.0036e-04	1.30	9.2610e-05	1.10	16.310

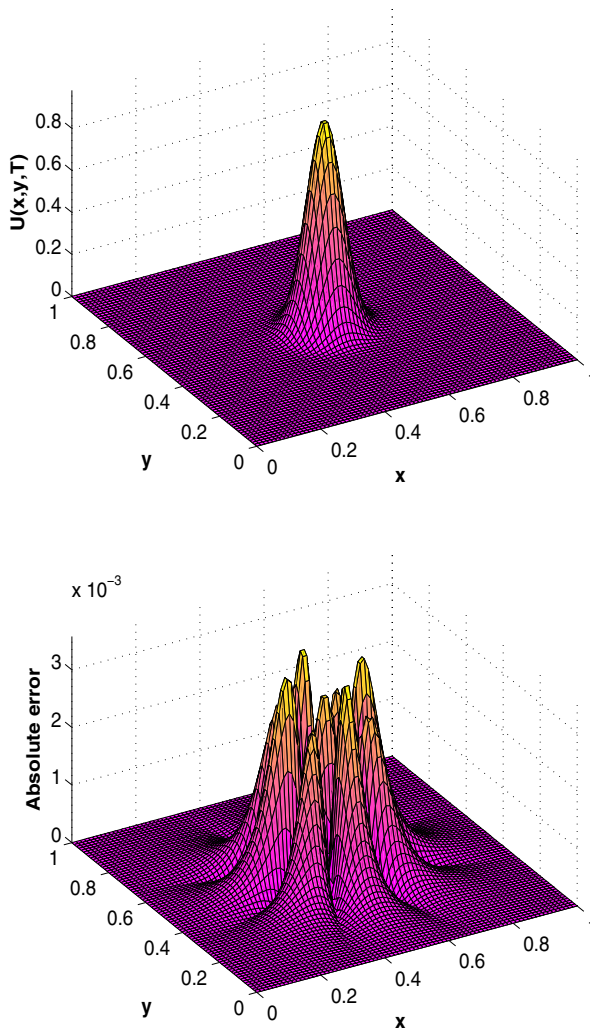


Fig. 6 Graph of numerical solution and absolute error for Example 2 with case II

Acknowledgements We would like to thank reviewers for their comments and suggestions that really improved the quality of the paper.

Compliance with Ethical Standards

Conflict of interest The authors declare that they have no conflict of interest.

References

1. Bagley, R.L., Torvik, P.: A theoretical basis for the application of fractional calculus to viscoelasticity. *J. Rheol.* **27**(3), 201–210 (1983)

2. Bhrawy, A., Abdelkawy, M.: A fully spectral collocation approximation for multi-dimensional fractional schrödinger equations. *J. Comput. Phys.* **294**, 462–483 (2015)
3. Cen, Z., Huang, J., Xu, A., Le, A.: Numerical approximation of a time-fractional black–scholes equation. *Comput. Math. Appl.* **75**(8), 2874–2887 (2018)
4. Chandhini, G., Prashanthi, K., Vijesh, V.A.: A radial basis function method for fractional darbox problems. *Engineering Analysis with Boundary Elements* **86**, 1–18 (2018)
5. Chen, W., Ye, L., Sun, H.: Fractional diffusion equations by the kansa method. *Comput. Math. Appl.* **59**(5), 1614–1620 (2010)
6. De Staelen, R., Hendy, A.S.: Numerically pricing double barrier options in a time-fractional black–scholes model. *Comput. Math. Appl.* **74**(6), 1166–1175 (2017)
7. Dehghan, M., Abbaszadeh, M.: Analysis of the element free galerkin (efg) method for solving fractional cable equation with dirichlet boundary condition. *Appl. Numer. Math.* **109**, 208–234 (2016)
8. Dehghan, M., Abbaszadeh, M.: Element free galerkin approach based on the reproducing kernel particle method for solving 2d fractional tricom-type equation with robin boundary condition. *Comput. Math. Appl.* **73**(6), 1270–1285 (2017)
9. Dehghan, M., Abbaszadeh, M.: Two meshless procedures: moving kriging interpolation and element-free galerkin for fractional pdes. *Appl. Anal.* **96**(6), 936–969 (2017)
10. Dehghan, M., Abbaszadeh, M.: The use of proper orthogonal decomposition (pod) meshless rbf-fd technique to simulate the shallow water equations. *J. Comput. Phys.* **351**, 478–510 (2017)
11. Dehghan, M., Abbaszadeh, M.: An efficient technique based on finite difference/finite element method for solution of two-dimensional space/multi-time fractional bloch–torrey equations. *Appl. Numer. Math.* **131**, 190–206 (2018)
12. Dehghan, M., Abbaszadeh, M., Mohebbi, A.: An implicit rbf meshless approach for solving the time fractional nonlinear sine-gordon and klein–gordon equations. *Engineering Analysis with Boundary Elements* **50**, 412–434 (2015)
13. Dehghan, M., Abbaszadeh, M., Mohebbi, A.: A meshless technique based on the local radial basis functions collocation method for solving parabolic–parabolic patlak–keller–segel chemotaxis model. *Engineering Analysis with Boundary Elements* **56**, 129–144 (2015)
14. Dehghan, M., Abbaszadeh, M., Mohebbi, A.: Analysis of a meshless method for the time fractional diffusion-wave equation. *Numerical Algorithms* **73**(2), 445–476 (2016)
15. Dehghan, M., Manafian, J., Saadatmandi, A.: Solving nonlinear fractional partial differential equations using the homotopy analysis method. *Numerical Methods for Partial Differential Equations: An International Journal* **26**(2), 448–479 (2010)
16. Dehghan, M., Mohammadi, V.: Two-dimensional simulation of the damped kuramoto–sivashinsky equation via radial basis function-generated finite difference scheme combined with an exponential time discretization. *Engineering Analysis with Boundary Elements* **107**, 168–184 (2019)
17. Dehghan, M., Safarpour, M., Abbaszadeh, M.: Two high-order numerical algorithms for solving the multi-term time fractional diffusion-wave equations. *J. Comput. Appl. Math.* **290**, 174–195 (2015)
18. Dehghan, M., Shokri, A.: A numerical method for solution of the two-dimensional sine-gordon equation using the radial basis functions. *Math. Comput. Simul.* **79**(3), 700–715 (2008)
19. Gao, G.H., Sun, Z.Z., Zhang, Y.N.: A finite difference scheme for fractional sub-diffusion equations on an unbounded domain using artificial boundary conditions. *J. Comput. Phys.* **231**(7), 2865–2879 (2012)
20. Ghehsareh, H.R., Bateni, S.H., Zaghian, A.: A meshfree method based on the radial basis functions for solution of two-dimensional fractional evolution equation. *Engineering Analysis with Boundary Elements* **61**, 52–60 (2015)
21. Ghehsareh, H.R., Zaghian, A., Raei, M.: A local weak form meshless method to simulate a variable order time-fractional mobile–immobile transport model. *Engineering Analysis with Boundary Elements* **90**, 63–75 (2018)
22. Golbabai, A., Nikpour, A.: Computing a numerical solution of two dimensional non-linear schrödinger equation on complexly shaped domains by rbf based differential quadrature method. *J. Comput. Phys.* **322**, 586–602 (2016)
23. Gu, Y., Zhuang, P.: Anomalous sub-diffusion equations by the meshless collocation method. *Aust. J. Mech. Eng.* **10**(1), 1–8 (2012)
24. Gu, Y., Zhuang, P., Liu, Q.: An advanced meshless method for time fractional diffusion equation. *Int. J. Comput. Methods* **8**(04), 653–665 (2011)

25. Hosseini, V.R., Chen, W., Avazzadeh, Z.: Numerical solution of fractional telegraph equation by using radial basis functions. *Engineering Analysis with Boundary Elements* **38**, 31–39 (2014)
26. Hosseini, V.R., Shivanian, E., Chen, W.: Local radial point interpolation (mlrpi) method for solving time fractional diffusion-wave equation with damping. *J. Comput. Phys.* **312**, 307–332 (2016)
27. Jin, B., Lazarov, R., Liu, Y., Zhou, Z.: The galerkin finite element method for a multi-term time-fractional diffusion equation. *J. Comput. Phys.* **281**, 825–843 (2015)
28. Kumar, A., Bhardwaj, A., Kumar, B.V.R.: A meshless local collocation method for time fractional diffusion wave equation. *Comput. Math. Appl.* **78**(6), 1851–1861 (2019)
29. Liu, Q., Liu, F., Turner, I., Anh, V., Gu, Y.: A rbf meshless approach for modeling a fractal mobile/immobile transport model. *Appl. Math. Comput.* **226**, 336–347 (2014)
30. Mardani, A., Hooshmandasl, M., Heydari, M., Cattani, C.: A meshless method for solving the time fractional advection–diffusion equation with variable coefficients. *Comput. Math. Appl.* **75**(1), 122–133 (2018)
31. Mohebbi, A., Abbaszadeh, M., Dehghan, M.: The use of a meshless technique based on collocation and radial basis functions for solving the time fractional nonlinear schrödinger equation arising in quantum mechanics. *Engineering Analysis with Boundary Elements* **37**(2), 475–485 (2013)
32. Mohebbi, A., Abbaszadeh, M., Dehghan, M.: Solution of two-dimensional modified anomalous fractional sub-diffusion equation via radial basis functions (rbf) meshless method. *Engineering Analysis with Boundary Elements* **38**, 72–82 (2014)
33. Nagy, A.: Numerical solution of time fractional nonlinear klein–gordon equation using sinc–chebyshev collocation method. *Appl. Math. Comput.* **310**, 139–148 (2017)
34. Quarteroni, A., Valli, A.: Numerical approximation of partial differential equations, vol. 23. Springer Science & Business Media (2008)
35. Salehi, R.: A meshless point collocation method for 2-d multi-term time fractional diffusion-wave equation. *Numerical Algorithms* **74**(4), 1145–1168 (2017)
36. Sarra, S.A.: A local radial basis function method for advection–diffusion–reaction equations on complexly shaped domains. *Appl. Math. Comput.* **218**(19), 9853–9865 (2012)
37. Sun, H., Liu, X., Zhang, Y., Pang, G., Garrard, R.: A fast semi-discrete kansa method to solve the two-dimensional spatiotemporal fractional diffusion equation. *J. Comput. Phys.* **345**, 74–90 (2017)
38. Sun, Z.Z., Wu, X.: A fully discrete difference scheme for a diffusion-wave system. *Appl. Numer. Math.* **56**(2), 193–209 (2006)
39. Tayebi, A., Shekari, Y., Heydari, M.: A meshless method for solving two-dimensional variable-order time fractional advection–diffusion equation. *J. Comput. Phys.* **340**, 655–669 (2017)
40. Uddin, M., Haq, S.: Rbfs approximation method for time fractional partial differential equations. *Commun. Nonlinear Sci. Numer. Simul.* **16**(11), 4208–4214 (2011)
41. Vong, S., Wang, Z.: A compact difference scheme for a two dimensional fractional klein–gordon equation with neumann boundary conditions. *J. Comput. Phys.* **274**, 268–282 (2014)
42. Yan, L., Yang, F.: Efficient kansa-type mfs algorithm for time-fractional inverse diffusion problems. *Comput. Math. Appl.* **67**(8), 1507–1520 (2014)
43. Yang, J., Zhao, Y., Liu, N., Bu, W., Xu, T., Tang, Y.: An implicit mls meshless method for 2-d time dependent fractional diffusion–wave equation. *Appl. Math. Model.* **39**(3–4), 1229–1240 (2015)
44. Zeng, F., Zhang, Z., Karniadakis, G.E.: Fast difference schemes for solving high-dimensional time-fractional subdiffusion equations. *J. Comput. Phys.* **307**, 15–33 (2016)
45. Zhuang, P., Gu, Y., Liu, F., Turner, I., Yarlagadda, P.: Time-dependent fractional advection–diffusion equations by an implicit mls meshless method. *Int. J. Numer. Methods Eng.* **88**(13), 1346–1362 (2011)